Isolation and characterization of novel temperate virus *Aeropyrum* globular virus 1 infecting hyperthermophilic archaeon *Aeropyrum*

Maho Yumiya[a], Yuto Fukuyama[b], Yoshihiko Sako[c], Takashi Yoshida[c]#

[a]Institute for Advanced Co-Creation Studies, Research Institute for Microbial Diseases, Osaka University, Yamadaoka, Suita, Osaka, Japan

[b]Research Center for Bioscience and Nanoscience, Japan Agency for Marine-Earth Science and Technology, Natsushima-cho, Yokosuka, Kanagawa Japan

[c]Laboratory of Marine Microbiology, Graduate School of Agriculture, Kyoto University, Kitashirakawa Oiwake-cho, Sakyo-ku, Kyoto Japan

Running title: Novel temperate virus infecting *Aeropyrum*

#Address correspondence to Takashi Yoshida

yoshida.takashi.7a@kyoto-u.ac.jp

Abstract word count:216

Word count for the main text:5673

ABSTRACT

We isolate a novel archaeal temperate virus named *Aeropyrum* globular virus 1 (AGV1) from the host *Aeropyrum* culture. Reproduction of AGV1 was induced by adding 20 mM tris-acetate buffer to exponentially growing host cells. Negatively stained virions showed spherical morphology (60 ±2 nm in diameter) similar to *Globuloviridae* viruses. The double-stranded circular DNA genome of AGV1 contains 18,222 bp encoding 34 open-reading frames. No ORFs showed significant similarity with *Globuloviridae* viruses. AGV1 shares three genes, including an integrase gene, with reported spindle-shaped temperate viruses. However we couldn't detect its integration site in the host genome. Moreover AGV1 seemed not to replicate autonomously because there are no origin recognition boxes in the genome. qPCR results showed that the genome copy number of AGV1 was lower than that of the host genome (10^{-3} copies per host genome). Upon the addition of tris-acetate buffer, a steep increase in the AGV1 genome copy number (9.5–26 copies per host genome at 2 days post-treatment) was observed although clustered regularly interspaced short palindromic repeat (CRISPR) elements of the host genome showed significant matches with AGV1 protospacers. Our findings suggest that AGV1 is a novel globular virus exhibiting an unstable carrier state in the growing host and in that way AGV1 can escape from the host defense system and propagate under stressful host conditions.

Importance

Studying archaeal viruses yields novel insights into the roles of virospheres and viruses in the evolutionary process of their hosts. Here, we isolated a novel spherical virus named *Aeropyrum*

globular virus 1. AGV1 has integrase gene but its genome is not integrated into the host genome. AGV1 could not replicate autonomously due to the lack of origin recognition boxes and thus its copy number was too low (10^{-3} copies per host genome) without any inducing stimulus. However, upon the addition of tris-acetate buffer, the AGV1 genome copy number steeply increased instead of a perfect sequence match between the spacer of the host CRISPR/Cas system and the protospacer. Our findings suggest that AGV1 can escape from the host defense system and propagate under stressful conditions for the host by establishing an unstable carrier state. These results reveals a novel aspect of host–virus interactions in extreme environments.

INTRODUCTION

Viruses are absolute intracellular parasites that depend on their host living organisms for replication(1, 2). Through infection, viruses can introduce genetic variation to the host microorganisms (3), affect their host microbial metabolism (4), directly kill their hosts by cell lysis, and accordingly contribute to the diversification of the microbial community (5). Virus–microorganism interactions also drive antagonistic coevolution that increases genetic diversity of both hosts and viruses (2). Thus, viruses are key players in microbial ecology (6).

Most *Crenarchaeota* members are hyperthermophiles that grow optimally at temperatures of at least 80°C. According to the International Committee on Taxonomy of Viruses, to date, cultured crenarchaeal viruses have been identified in 13 genera, such as *Sulfolobus, Acidianus, Stygiolobus, Thermoproteus, Pyrobaculum,* and *Aeropyrum* (7). Crenarchaeal viruses exhibit diverse morphologies, including spindle-shaped and bottle-shaped cells, which have never been reported

71 in other domains of life (7-9). The life cycles of viruses are largely divided into lytic and lysogenic
72 cycles (10). However, to adapt to the harsh conditions of the host habitat, crenarchaeal viruses,
73 except for lytic viruses, e.g., *Thermoproteus tenax* virus 1 (11), *Sulfolobus* turreted icosahedral
74 virus (12) and *Acidianus* two-tailed virus (13), do not exhibit typical lytic cycles and develop a
75 carrier state in their host. Viruses in carrier state represent a harmonious coexistence with host
76 species and propagate without genome integration and cell lysis (8). It is considered that carrier
77 state is unique and significant strategy for viruses infecting *Crenarchaeota.* All members of
78 *Fuselloviridae* (14)*, Guttaviridae* (15, 16)*,* and *Bicaudaviridae* (13) are lysogenic viruses and
79 possess integrase genes. Some of them can not only integrate their circular genome into host
80 chromosomes (17) but also establish carrier state. The archaeon *Sulfolobus shibatae* B12 is the
81 natural host of the fusellovirus *Sulfolobus* spindle-shaped virus 1 (SSV1), which exists in episomic
82 and integrated forms. SSV1 can propagate at low levels (10^7 virus particles/mL) without cell lysis
83 and even in the absence of an inducing stimulus (18). Thus, its lysogenic cycle is a model of carrier
84 state (19). Transcriptomic analysis of SSV1-infected cells suggests that the virus tightly represses
85 gene expression during its carrier state to establish an equilibrium between viral replication and
86 cellular multiplication (20). However, owing to the limited number of cultured viruses and unique
87 genomic contents, knowledge on the mechanisms and the ecological effects of the carrier state is
88 limited.
89
90 Belonging to the phylum *Crenarchaeota, Aeropyrum* spp. are aerobic, neutrophilic, and
91 heterotrophic hyperthermophiles (21). There are only two closely related *Aeropyrum* species,
92 *Aeropyrum pernix* (21) and *Aeropyrum camini* (22). Four viruses that infect *A. pernix* have been
93 isolated and described: *Aeropyrum pernix* bacilliform virus 1 (APBV1) (23), *Aeropyrum pernix*

94 ovoid virus 1 (APOV1) (15), *Aeropyrum pernix* spindle-shaped virus 1 (APSV1) (15), and
95 *Aeropyrum* coil-shaped virus (ACV) (24). APBV1 and ACV are the first members of Clavaviridae
96 and Spiraviridae, respectively (23, 24). Further diversity in *A. pernix* viruses was predicted to have
97 been still veiled in hot environments by transmission electron micrograph (TEM) observations
98 (e.g., filamentous virus and short bacilliform virus) (23). *Aeropyrum* species are specialists in their
99 habitat requirements and possess small and very conservative genomes (25). Genomic variation is
100 observed in virus-related elements including two proviral regions (*Fuselloviridae* APSV1 and
101 *Guttaviridae* APOV1), adaptive immune system against foreign genetic elements (clustered
102 regularly interspaced short palindromic repeat [CRISPR]), and ORFans probably originating from
103 viruses (25). In addition, most spacer sequences (141/144) in the CRISPR loci of *A. pernix* K1 and
104 *A. camini* SY1 showed no similarity to databases (25). It is considered that their genomic
105 diversification is mostly derived from viruses and that there are unknown viruses interacting with
106 *A. pernix* and contribute to their population dynamics in the environment.
107 Here, we report the isolation of a novel temperate virus infecting *Aeropyum* species and
108 investigate how the virus establish its unique carrier state in the host culture using quantitative
109 PCR assay.
110

111 **MATERIALS AND METHODS**

112 **Sample collection.** On December 12, 2012 and May 27, 2014, samples were collected from the
113 Yamagawa coastal hydrothermal field (31°10'58″ " N, 130°36'59"″ E) in the Kagoshima Prefecture.
114 Effluent seawater and coastal sand were collected using a ladle and stored in 50 mL centrifuge
115 tubes (Greiner Bio-One, frickenhausen,Germany). All tubes were transported in ice packs to the
116 laboratory by a refrigerated courier service (Yamato Transport, Tokyo, Japan) and stored at 4°C

117 until use.

118

119 **Isolation of the host strain.** To establish the enrichment culture of *A. pernix,* approximately 0.5 g
120 sample collected from 2012 was inoculated into the 5 mL JXTm medium (1 g tryptone, 1 g yeast
121 extract, 28.15 g NaCl, 0.67 g KCl, 5.51 g $MgCl_2 \cdot 6H_2O$, 6.92 g $MgSO_4 \cdot 7H_2O$, 1.45 g $CaCl_2$, and 1
122 g $Na_2S_2O_3 \cdot 5H_2O$ per liter, pH 7.0) (26) in 18 × 180 mm hermetically sealed screw-cap test tubes.
123 The cultures were incubated at 90°C in a dry oven (FC612 or DRS620DB; ADVANTEC, Tokyo,
124 Japan) under atmospheric conditions. Then, the enriched cells were streaked onto a ST Gelrite
125 plate (containing 32 g of sea salt (Sigma Aldrich, St. Louis, Missouri, USA), 1 g $Na_2S_2O_3$ $5H_2O$,
126 0.8 g yeast extract (Becton, Dickinson and Company, Franklin Lakes, New Jersey), 1.2 g tryptone
127 (Becton, Dickinson and Company, Franklin Lakes, New Jersey, USA), and 8 g Gelrite gellan gum
128 (Sigma Aldrich, St. Louis, Missouri, USA) per liter) in glass Petri dishes (10 cm in diameter). The
129 plates were incubated at 90°C in a BBL GasPak™ 100 Holding Jar (Becton, Dickinson and
130 Company, Franklin Lakes, New Jersey, USA) to avoid evaporation. After 3 to 5 days of incubation,
131 well-isolated colonies formed on the surface of the plates were collected and transferred to a fresh
132 JXTm medium. To ensure the purity of the *Aeropyrum* isolate, the streaking and isolation steps
133 were repeated at least three times, and the 16S rRNA gene sequences and four housekeeping genes
134 (*pheS, radA, gap,* and *ast*) were confirmed using Sanger sequencing performed using a BigDye
135 Terminator v3.1 Cycle Sequencing Kit on Applied Biosystems 3130 genetic analyzer
136 (ThermoFisher Scientific, Waltham, Mssachusetts, USA). The isolate was designated as the host
137 strain, *A. pernix* YK1-12-2013.

138

139 **Virus culture and isolation.** Approximately 5 g sample collected in 2014 were inoculated into

140 fresh 1,000 mL JXTm medium in 2000 mL Erlenmeyer flasks sealed with silicone plug and
141 incubated as described above. After 3 days, samples were centrifuged at 5,000 × g for 30 min in
142 500-ml Nalgene™ PPCO centrifuge bottles (ThermoFisher Scientific, Waltham, Mssachusetts,
143 USA) at 4°C, and NaCl and polyethylene glycol 6000 were added to the supernatant (final
144 concentration: 1 M and 10%, respectively). After incubation at 4°C overnight, viral particles were
145 collected by centrifugation at 12,000 × g for 30 min at 4°C and suspended in 10 m: virus storage
146 buffer (20 mM Tris-acetate at pH 7.0 containing 3.0% sodium chloride) and designated as the
147 environmental virus fraction.

148 To screen viruses infecting A. *pernix* YK1-12-2013, we inoculated the 10 mL
149 environmental virus fraction with 1,000 mL exponentially growing *A. pernix* YK1-12-2013 culture
150 in 2000 mL Erlenmeyer flasks. As a control and mock treatment, we added virus suspension buffer
151 and JXTm medium to the culture medium. Viral fractions were prepared as described above after
152 further growth for approximately four days. Virus propagation was verified using transmission
153 electron microscopy (TEM) as described below. For further purification, 10 mL chloroform was
154 added. After vigorous vortexing, the suspension was centrifuged (7,500 ×g, 4°C, 20 min), and the
155 aqueous layer was layered on a CsCl step-gradient (1.15, 1.25, and 1.40 g ml^{-1}) and purified by
156 CsCl step-gradient ultracentrifugation at 107,000×g for 60 min at 15°C using a Beckman Coulter
157 Optima L-80 ultracentrifuge, SW41Ti rotor (Beckman Coulter Inc, Brea, California, USA). The
158 concentrated viruses were collected using a 26-gauge needle and dialyzed in 500 mL SM buffer
159 (50 mM Tris-HCl, 100 mM NaCl, 10 mM $MgSO_4 \cdot 7H_2O$, 0.01% gelatin) at 4°C overnight.

160

161 **TEM analysis.** For negative staining, 5 μL samples were applied to carbon-coated copper grids
162 (Nisshin EM, Tokyo, Japan) stained with 2% uranyl acetate for 5–10 s. They were visualized using

163 an H-7650 (Hitachi, Tokyo, Japan) at 80 kV at magnifications of 10,000× to 40,000×.

164

165 **DNA extraction, sequencing, and host and viral genome assembly** Extraction of cellular DNA
166 and viral DNA was conducted using Wizard® Genomic DNA Purification Kit (Promega, Madison,
167 Wisconsin, USA) and QIAamp MinElute viral DNA extraction kit (QIAGEN, Venlo, Netherland),
168 respectively, following the manufacturer's protocol. The sequencing library was prepared using a
169 Nextrera XT library preparation kit (Illumina, San Diego, California, USA), and genomes were
170 sequenced on the Illumina MiSeq v2 system with paired-end reads. The sequence of the viral
171 genome was technically replicated (n = 2, defined as VL1 and VL2). We eliminated the reads with
172 a Phred score below Q30 for 90% of the bases using the FASTQ Quality Filter of FASTX-Toolkit
173 (http://hannonlab.cshl.edu/fastx_toolkit/). The reads were assembled using the Velvet Optimiser
174 ver. 2. 2. 5 (http://bioinformatics.net.au/software.velvetoptimiser.shtml) (27).

175 To obtain the complete viral genome, VL1 and VL2 were assembled. We searched for
176 homologous sequences between the VL1-contigs and VL2-contigs using the BLASTN program at
177 the National Center for Biotechnology Information (NCBI) and assembled the contigs sharing
178 significant homologous sequences using MEGA7 (28). If the length of the homologous sequence
179 was less than 200 bp, the integrity of the assembly was confirmed using PCR. Finally, the gaps
180 between the contigs were bridged using Sanger sequencing of the PCR products.

181

182 **Genome analysis.** Open reading frames (ORFs) were predicted using the Microbial Genome
183 Annotation Pipeline (MiGAP) (29) following manual curation. To determine the homology of
184 ORFs to known proteins, we searched for non-redundant database protein sequences in the NCBI
185 database using BLASTP (as of March 2021, E = 1e-5). Searches for conserved protein domains

186 were performed using HMMscan (30) against Pfam (31) (as of March 2021. *E* = 1e-5). Membrane-
187 spanning regions were predicted using the TMHMM ver. 2.0
188 (http://www.cbs.dtu.dk/services/TMHMM/) (32). Circular genome maps and GC skew
189 calculations were performed using DNAPlotter (33). Genome alignments with related viruses
190 based on genome-wide sequence similarities computed by tBLASTx were drawn using ViPTree
191 web server version 1.9 (http://www.genome.jp/viptree/) (34).
192 To determine the AGV1-integration site in the host genome, we searched for homologous
193 sequences between the virus genome and the *A. pernix* YK1-12-2013 draft genome using BLASTN.
194 To ensure high sensitivity, sequence reads of the host were mapped onto the viral genome using
195 Bowtie2 (35). The CRISPR elements and spacers were identified using CRISPRFinder (36) with
196 manual validation. The virus genome was searched against the spacers registered in the CRISPRs
197 database (as of March 2021) and the identified spacers of *A. pernix* YK1-12-2013 using BLASTN
198 optimized for somewhat similar sequences.
199
200 **Protein analysis of virus.** Purified virions were incubated at 95°C for 20 min with the buffer
201 solution without the reducing reagent (6x) and subjected to SDS-PAGE (12% polyacrylamide gel;
202 80 × 90 × 1.0 mm; 200V; Nacalai Tesque, Kyoto, Japan) using ATTO AE-6450 mini PAGE system
203 (ATTO, Tokyo, Japan). Proteins were transferred onto an Immobilon P membrane (Millipore,
204 Burlington, Massachusetts, USA) using TRANS-BLOT SD SEMI DRY TRANSFER CELL (Bio-
205 Rad, Hercules, California, USA) at 180 mA for 80 min and stained with CBB Stain One (Nacalai
206 Tesque, Kyoto, Japan). A protein ladder (Nacalai Tesque, Kyoto, Japan) with molecular masses
207 ranging from 10 to 250 kDa was used. The major protein band was excised using a scalpel, and
208 the N-terminal amino acid sequence was determined by Edman degradation (APRO Science,

209 Tokushima, Japan).

210

211 **Growth kinetics analysis of virus.** We monitored the cellular (16S rDNA) and viral (integrase)
212 genome copy numbers using qPCR. *A. pernix* YK1-12-2013 (1,000 mL culture) was grown in
213 2,000 mL Erlenmeyer flasks sealed with silicone plugs at 90°C without shaking. After 24 h
214 incubation, 10 mL viral fraction or virus storage buffer (control; 20 mM Tris-acetate at pH 7.0
215 containing 3.0% sodium chloride) was added to *A. pernix* YK1-12-2013 cultures, and 10 mL was
216 sampled every 24 h. For each sample, *A. penix* YK1-12-2013 was collected as described above.
217 Virions were collected by ultracentrifugation at 25,000 rpm for 90 min at 4°C using a Beckman
218 Coulter Optima L-80 ultracentrifuge, SW41Ti rotor. Cellular DNA and viral DNA were extracted
219 from the cell-free supernatant by using kits as described above, and qPCR was performed for
220 quantification. For the archaeal 16S rRNA gene, primer sets 931f-m1100r were used (37). The
221 primers for the viral integrase gene were designed to target the 226-bp internal region of the
222 integrase gene (Table 1). Standards used to determine the gene copy numbers of the 16S rRNA
223 and integrase genes were prepared using the genomic DNA from *A. pernix* YK1-12-2013 and the
224 purified virus, respectively. qPCR was performed using SYBR Premix Ex Taq II (Tli RNaseH
225 Plus) (TaKaRa Bio, Shiga, Japan) on a TaKaRa PCR thermal cycler Dice® real-time system single
226 and software. Thermal cycler Dice Real Time System Single (ver. 4.02 B for TP850) was used for
227 the calculation of Ct values, generation of standard curves, and analysis of dissociation curves.
228 Each PCR mixture (20 μL per tube) contained primers and SYBR® Green Ⅰ solution of the
229 recommended concentration according to the manufacturer's guidelines. The PCR protocol for
230 16S rRNA genes was as follows: 60 s at 95°C for initial denaturation, 45 cycles of 5 s at 95°C, 10
231 s at 64°C, and 30 s at 72°C. The PCR protocol for integrase genes was as follows: 60 s at 95°C for

232 initial denaturation, 45 cycles of 10 s at 95°C, 15 s at 61°C, and 40 s at 72°C. Dissociation curves
233 were generated by gradually increasing the temperature from 60°C to 95°C after the PCR cycle.
234
235 **Growth analysis of host.** The effect of viral infection on *A. pernix* YK1-12-2013 growth was
236 confirmed using culture-turbidity measurements. Briefly, 100 μL AGV1 fraction, virus storage
237 buffer, or JXTm was added to exponentially growing host cells in 5 mL culture in 18 × 180 mm
238 hermetically sealed screw-cap test tubes. Every 8 h, 100 μL of culture was collected, and OD_{600}
239 was measured using Ultrospec 3100 pro (GE Healthcare, Chicago, Ilinois, USA).
240
241 **Virus induction assay.** Cells were grown in 5 mL culture in 18 ml screw-capped test tubes at 90°C
242 without shaking for 24 h. To determine the factor inducing AGV1 replication, we performed stress
243 treatments on *A. pernix* YK1-12-2013 cultures. First, pH was changed from 7.0 to 6.0 by adding
244 3M acetate. Second, exponentially growing host cells were transferred to shallow plastic dishes
245 and subjected to UV irradiation at 254 nm for 30 s using a BioRad GS gene linker (BioRad,
246 Hercules, California, USA). Third, we shifted the cultivation temperature from 90°C to 80°C.
247 Fourth, 100 μL 5 M NaCl was added. Lastly, 100 μL 0.25 M EDTA (pH 7.0) was added. For each
248 culture, cells were collected 48 h post-treatment, and cellular DNA was extracted and used as a
249 PCR template to confirm AGV1 induction.
250
251 **Host range analysis.** Host analysis was conducted using the following strains: *A. pernix* K1 and
252 *A. camini* SY1 obtained from the Deutsche Sammlung von Mikroorganismen und Zellkulturen
253 (DSMZ, Braunschweig, Germany) as DSMZ 11879 and DSMZ 16960, respectively, and three *A.*
254 *pernix* laboratory strains isolated from various hydrothermal fields: OH2, TB7 (26), and FT1-29-

255 2014 (from Shimogamo hot spring, Shizuoka, Japan).

256 Each strain was inoculated with 100 μL AGV1 fraction growing in 5 mL medium JXTm
257 (defined as culture A) for 2 d. Then, 100 μL culture A was transferred to 5 mL fresh medium and
258 incubated for another 2d twice (defined as cultures B and C). Genomic DNA was extracted from
259 cultures A, B, and C per strain. Using these DNA templates, qPCR was performed using AGV1-
260 specific primers to confirm infection. PCR using 16S rRNA-specific primers was used as the
261 control.

262

263 **Data availability.** The AGV1 genome and *A. pernix* YK1-12-2013 draft genome sequences have
264 been deposited in the DNA Data Bank of Japan (DDBJ) database under the accession numbers
265 LC208019 and BDMD01000001-BDMD010000144, respectively.

266

267 **RESULTS & DISCUSSION**

268 **Isolation of novel temperate virus.** An enrichment culture was established from samples
269 collected from a hydrothermal field in Kagoshima, Japan, wherein *Aeropyrum* species and their
270 infectious viruses have been previously isolated (26). From the TEM images, we observed spindle-
271 shaped, pleomorphic, and linear virus-like particles in a viral fraction prepared from the
272 enrichment culture (data not shown). To isolate the infectious viruses of *A. pernix*, the viral fraction
273 was inoculated with *A. pernix* YK1-12-2013. After 4 days, host growth retardation was detected,
274 and spherical particles approximately 60 ± 2 nm in diameter were observed in viral fractions from
275 the cultures inoculated with virus fraction. And the same particles were also observed in viral
276 fraction from culture added with virus storage buffer (Figs. 1). No virus-like particles were
277 observed in the supernatant of *A. pernix* YK1-12-2013 cell culture without viral fraction or virus

278 storage buffer. These observations indicate that the spherical viral particles are derived from a
279 temperate virus (or viruses) within the *A. pernix* YK1-12-2013 strain.

280 The spherical virions are morphologically similar to those belonging to the *Globuloviridae*
281 family, i.e., *Pyrobaculum* spherical virus 1 (38) and *Thermoproteus tenax* spherical virus 1 (39).
282 Neither surface structures nor tails were observed. As there has been no reports to date on a
283 spherical virus infecting *Aeropyrum* and we successfully obtained a single circular genome from
284 these spherical virions later, we described these isolates as a novel virus species infecting
285 *Aeropyrum* named *Aeropyrum* globular virus 1 (AGV1).

286

287 **AGV1 genomic features of and host genomic interactions.** A single circular dsDNA genome
288 containing 18,222 bp (Fig. 2A and Table 2) was assembled from spherically shaped particles. We
289 numbered the nucleotides in the genome sequence beginning from the start codon of the first ORF
290 following the replication origin. The ORFs are correspondingly numbered and the following
291 number refers to the number of amino acids in the predicted protein (e.g. ORF1_309). The GC
292 content (55.8%) was similar to those of host chromosomes (50.7–56.7%) (25) and the reported
293 dsDNA viruses infecting *A. pernix* (52.7–56.5%) (15, 23)) but higher than those of other spherical
294 viruses PSV (48%) (38) and TTSV (49.8%) (39). The AGV1 genome encoded 34 predicted ORFs
295 starting from the ATG, GTG, and TTG codons (Table 3). Of these, 27 (79.4%) were present in one
296 DNA strand, and only 7 were present on the other. The GC skew analysis revealed that the origin
297 of replication is most likely located in the intergenic region between ORF 1_309 and ORF 34_215.
298 We detected an inverted repeat, 5′-CACCCTGCTCTACTATAGTCTAT – N_{93}–
299 ATAGACTCTATAGTAGAGCCAGGGTG –3′ in this region. The *oriC* sites on the *A. pernix* K1
300 genome contain crenarchaeal origin recognition boxes (ORBs) which are the binding sites for

301 Orc1/Cdc6 proteins and ori-specific uncharacterized motifs (UCMs), an important signature motif
302 in the center of origin in *Aeropyrum* (40). We did not find any ORBs or UCMs around the putative
303 replication origin on the AGV1 genome, suggesting that AGV1 cannot replicate autonomously.
304 Of the predicted ORFs, 10 (29.4%) showed significant similarity to the genes in the nr database
305 (Table 3). SDS-PAGE revealed a single major protein band of approximately 28.5 kDa from the
306 protein fraction extracted from purified AGV1 virions (Fig. 2B), 5 N-terminal amino acid
307 sequences of which completely matched with the internal amino acid sequences of a protein
308 encoded by AGV1 ORF1_309. According to the HMMscan (30) analysis, 12 (35.3%) ORFs
309 showed similarity to the protein domains registered in the Pfam database (31). We collectively
310 assigned functions to these 13 AGV1 gene products (Fig. 2A, Table3).

311 PSV1 and TTSV1, the reported members of *Globuloviridae*, share 15 genes including two
312 structural proteins (39). Although AGV1 virions are morphologically similar to PSV1 and TTSV1,
313 the structural protein of AGV1 showed no similarity with those of PSV1 and TTSV1. Moreover,
314 no homologs were found on the AGV1 genome. The five AGV1 genes showed significant
315 similarities with those of reported crenarchaeal temperate viruses. Particularly, three of the five
316 genes are similar to that in Fuselloviruses, namely integrase (ORF 26_339) in the SSV-like region
317 on *Sulfolobus islandicus* M.16.4, nuclease (ORF 21_191) in SSV2, and putative transcriptional
318 regulator (ORF 22_70) in APSV1. Integrase genes found in archaeal extrachromosomal elements
319 are classified into two types: SSV1-type and pNOB8-type (40). AGV1 integrase is an SSV1-type
320 integrase, a kind of tyrosine recombinase catalyzing the site-specific integration and excision of
321 the viral genome (40). HMMS revealed that the functional domain was conserved in the integrase
322 gene. We found that the $tRNA^{Glu}$ gene was inserted in the AGV1 integrase gene sequence,
323 suggesting that $tRNA^{Glu}$ is the integration site of the integrase. Furthermore, ORF22_70 products

324 encoded a putative DNA-binding protein containing the ribbon-helix-helix (RHH) domain
325 common to the CopG family. This domain was also predicted for the ORF15_146 product. The
326 RHH domain protein is one of the most conserved proteins in archaeal viruses (41) and recognizes
327 target sequences in the DNA by forming dimers and inserting them into the groove (42). The RHH
328 domain was also found in F55, which tightly regulates the SSV1 lysogenic state (20) and is
329 involved in controlling plasmid copy numbers (42).

330 Four ORFs of AGV1 were homologs of *Aeropyrum*-encoded genes, three of which
331 (ORF18_111, ORF22_70, and ORF31_258) are shared with the provirus on the *A. pernix* K1
332 genome. AGV1 shares a hypothetical protein (ORF18_111) and putative glutamyl $tRNA^{Glu}$
333 reductase (ORF31_258) with APOV1.

334 Five ORFs showed sequence similarity to those of other hyperthermophilic crenarchaeota,
335 including trypsine-like peptidase (ORF4_262), nuclease (ORF21_191), and ATP-binding
336 protein(ORF28_309) in *Pyrodictium* sp.; pillin(ORF 20_141) in *Thermogladius calderae*; and
337 hypothetical protein (ORF33_330) in *Thermoprotei archaeon*. Trypsine-like peptidase is also
338 encoded by the ssDNA virus ACV (24) and might be involved in the release or invasion cycle of
339 these viruses.

340 ORF28_309 exhibited a P-loop containing region of the AAA domain, which is conserved
341 among the ATP- or GTP-binding proteins and is encoded by many archaeal viruses (43). Typically,
342 viral P-loop proteins are nucleic-acid-stimulated ATPases that are involved in viral replication,
343 transcription, or packaging and are related to bacterial DnaA (43). We found that 13 ORFs,
344 including structural proteins and pilli, exhibit one to four transmembrane motifs predicted by the
345 TMHMM 2.0 program.

346 Finally, we compared the AGV1 genome with those of related crenarchaeal viruses on a

347 genome-wide scale using ViPTree (34). AGV1 shared some genes with APOV1 and *Fuselloviridae*
348 members, but most of its genomic content was unique, indicating the novelty of AGV1. The
349 genome architecture of AGV1 showed mosaicism, which may reflect the genetic exchange among
350 other viruses and organisms. Genome mosaicism of viruses has been reported between bacterial
351 phages and archaeal head-tail viruses. To date, there have been no reports on viruses infecting
352 crenarchaeota (9, 44).
353
354 To predict the AGV1 integration site on the host genome, we performed a draft genome
355 sequence analysis of the host. The draft assemblies of the *A. pernix* YK1-12-2013 genome yielded
356 144 contigs with an average GC content of 56.5% (Table 2). The draft genome was approximately
357 1.6 Mbp long, and a total of 1,727 ORFs were identified. However, we could not detect the AGV1
358 integration site in the host genome or any sequence reads of the host mapped to the AGV1 genome,
359 including $tRNA^{Glu}$. That is to say, the read coverage of the AGV1 genome was lower than that of
360 the host genome indicating that AGV1 was harbored by some host cells in culture. APOV1 and
361 APSV1 harbor the SSV1-type integrase and are integrated into the chromosome of the host *A.*
362 *pernix* K1 (15). In addition, *Fuselloviridae* members encode SSV1-type integrases and are
363 integrated into the host chromosome (40). In contrast, *Bicaudaviridae* members, which also carry
364 the SSV1-type integrase but integration of viral genome has not yet been reported except for
365 ATV(13). Furthermore, a recent study revealed that the integrase gene is not essential for SSV1
366 (45); thus, genome integration is not always essential for infection. We obtained a pure host cell
367 culture using previous methods (22, 26) and confirmed no redundancy of 16S rRNA genes and
368 housekeeping genes by Sanger sequencing and draft genome sequencing (data not shown but the
369 sequences obtained by Sanger sequencing completely matched those of the draft genome).

370 Therefore, we presumed that AGV1 is not integrated into the host genome and maintained as a
371 episome in the host cell and that initially, the host culture consisted of only AGV1-carrying cells,
372 but AGV1-carrying cells were diluted upon host cell division as AGV! could not replicate
373 autonomously due to the lack of the ORBs or UCMs.
374
375 **Virus-host relationship.** To confirm the maintenance and replication of the AGV1 genome in host
376 cells, we monitored the host/virus genome copy numbers during infection. AGV1 genome copy
377 number was 5.6 to 35 × 10^3 times lower than that of host genome, and replication did not occur
378 without induction stimulus (Fig. 3). At 9 h post-treatment, AGV1 in the host cells rapidly increased.
379 At 48 h post-treatment, its genome copy number reached approximately 3 to 5 × 10^8 copies mL^{-1}
380 culture and exceeded that of host genomes by 9.5 to 26-fold. The AGV1 genome copy number in
381 the supernatant exhibited a similar increasing pattern and plateaued at approximately 3×10^7 copies
382 mL^{-1} culture at 72 h post-treatment. When it plateaued, AGV1 virions were observed in the cell
383 free supernatant by TEM.
384 To clarify whether AGV1 infection affects host growth, we monitored host growth with or
385 without AGV1 and under AGV1-induced conditions. Host growth was more significantly retarded
386 following AGV1 inoculation than under AGV1-induced conditions. Growth retardation was
387 observed immediately after AGV1 inoculation and 12 h post-induction, at which AGV1
388 propagation in the host cell started (Fig. 4). Infection with AGV1 did not lead to host cell lysis as
389 evidenced by a lack of decrease in OD_{600} and the absence of cell debris in the culture of infected
390 cells.
391
392

393 ***Aeropyrum*–AGV1 interaction via the CRISPR/Cas system.** CRISPR is a microbial adaptive
394 immune system that cleaves foreign genetic elements (46). CRISPR allows cells to specifically
395 recognize the target sequences using spacers acquired from the proto-spacer (small DNA segment
396 of invaders) and inhibits viral infection, such as RNA interference manner (47). To investigate the
397 AGV1–host interaction via CRISPR, we identified the CRISPR loci on the host genome and
398 spacers originating from AGV1. *A. pernix* YK1-12-2013 carried two CRISPR loci (Apyk_1 and
399 Apyk_2) carrying 39 and 57 repeat-spacer units, respectively.

400 We detected *cas*2 and *cas*4 genes adjacent to Apyk_2. *cas2* and *cas4* genes are important
401 for insertion of spacers into CRISPR arrays. We also detected other *cas* genes involved in spacer
402 acquisition (*cas1*), target binding (*csa2, cas5, cmr2,* and *cmr3*), and target cleavage (*cmr4, cmr6,*
403 *and csx1*) in the draft genome (46). Direct repeat sequences and leader sequences of Apyk_1 and
404 Apyk_2 were matched to the repeat sequences of Ape_1 and Aca_2 (25), which are previously
405 reported CRISPR loci of *A. pernix* K1 and *A. camini* SY1, respectively. We found 8 protospacers
406 on AGV1 (Table 4), 3 of which matched those on the CRISPR loci on the *A. pernix* YK1-12-2013
407 genome, whereas the remaining five matched those of *A. pernix* K1. The sequence of the single
408 spacer (Apyk_2_45) perfectly matched that of the protospacer. Other protospacers had at least one
409 nucleotide mutation.

410 Next, the nucleotide mutations in the protospacers were examined to determine whether
411 they caused synonymous substitutions. We found that most nucleotide mutations caused
412 synonymous substitutions, except for Apyk_2_35. Apyk_2_35 contains a single amino acid
413 substitution of isoleucine to valine; however, this residue was conserved, suggesting an arms race
414 between AGV1 and the host. Our results suggest that CRISPR protects *A. pernix* YK1-12-2013
415 from AGV1 infection.

416 Recent transcriptomic analysis of *S. solfataricus* infected with two closely related
417 temperate viruses, SSV1 and SSV2, indicates that CRISPR interacts with the temperate virus and
418 regulates its copy number (19). SSV2 showed a steep increase in copy number (from to 1–3 to 25–
419 50 copies per cell) during host growth (48) and elicited a strong host response, including CRISPR
420 (19). On the other hand, SSV1 maintained its copy number at a low level without any induction
421 stimulus (18) and did not activate the host defense system (19). Furthermore, viruses with
422 destructive effects on the host induce a stronger host defense response as evidenced by the high
423 numbers of spacer matches to lytic virus ATV found in the CRISPR loci of *S. solfataricus* P2
424 compared with carrier-state viruses (e.g., fuselloviruses infecting the strain) (9). Thus, we assumed
425 that the CRISPR/Cas immunity of *A. pernix* YK1-12-2013 represses AGV1 propagation because
426 high concentrations of AGV1 might have damaging effects on host growth. Alternatively, AGV1
427 might be in the cryptic phase during the optimal growth phase of the host to escape from the host
428 defense. However, AGV1 can propagate steeply upon certain stress stimuli, such as addition of the
429 virus storage buffer. The detailed mechanism of AGV1 life cycle remains to be elucidated.
430
431 **Factors associated with AGV1 induction.** To identify the AGV1 induction stimulus, we
432 examined AGV1 propagation under various stress conditions. PCR products of AGV1 were
433 obtained in cells growing under stress conditions stimulated, namely suboptimal growth pH,
434 suboptimal growth temperature, and UV irradiation (Fig. 5) besides tris addition. Salinity shift and
435 addition of chelating agent didn't induce AGV1 propagation. AGV1 genome copy number was
436 approximately measured as 1×10^3 copies mL^{-1} cultures under suboptimal growth pH, suboptimal
437 growth temperature and UV irradiation. The addition of tris-acetate buffer induced approximately
438 1×10^8 copies mL^{-1} and was the most effective stimulus to induce AGV1 propagation.
439

440 **Host range analysis.** The host range of AGV1 was evaluated by inoculating AGV1 with
441 exponentially growing cells of five *Aeropyrum* strains isolated from various hydrothermal fields
442 in Japan. We did not detect the AGV1 genome in all cultures of OH2, TB7, and FT1-29-2014
443 strains. In *A. pernix* K1, we detected the AGV1 genome at a low level (4.8 to 7.0 × 10^2 copies mL^{-}
444 ^{1}) in cultures A and C. In *A. camini* SY1, we detected the AGV1 genome at 1.0 × 10^6 copies mL^{-1}
445 in culture B and at 5.5 × 10^6 copies mL^{-1} in culture C. 16S rRNA gene was detected in all cultures
446 at approximately 10^5 copies mL^{-1}.

447 Thus, *A. pernix* K1 and *A. camini* SY1 could be infected by AGV1. We continued to
448 subculture both AGV1-infected strains and after 10-time subculturing, we performed qPCR
449 targeting AGV1 integrase. However, we could not detect the AGV1 genome in cultures with or
450 without the virus storage buffer. Similarly, the *Sulfolobus neozealandicus* droplet-shaped virus
451 belonging to *Guttaviridae* was found in an unstable carrier state (16). In contrast, we did not obtain
452 any AGV1-free strain of the native host, *A. pernix* YK1-12-2013, despite long-term subculturing
453 and effort to curation by plating and limiting dilution. Elucidation of the detailed mechanism
454 should be explored in future studies.

455

456

457 Overall, we successfully isolated a novel spherical temperate virus AGV1 that infects the
458 hyperthermophilic archaeon *Aeropyrum*. AGV1 was morphologically similar to *Globuloviridae*
459 viruses but doesn't share any genes with them. According to the genetic information, AGV1
460 seemed to be a temperate virus but AGV1 couldn't neither integrate into the host genome nor
461 replicate autonomously. On the other hand, AGV1 could propagate with inducing stimulus in spite
462 of threat of the host CRISPR/Cas system. Although an "unstable carrier state" of AGV1 seemed

463 to be disadvantageous for the survival, it might be a reasonable way to adapt to the host defense
464 system and the harsh environment of the host habitat. We hypothesize AGV1 could hides from
465 host defense system by unstable carrier state without inducing stimulus and propagate steeply on
466 detecting stressful condition for its host. These results and hypothesis shed new light on virus-host
467 interaction under extreme environment.
468

469 **ACKNOWLEDGMENTS.** Computational analysis was performed at the Super Computer
470 System, Institute for Chemical Research, Kyoto University. We thank the Center for Anatomical,
471 Pathological, and Forensic Medical Researches (Graduate School of Medicine, Kyoto University)
472 for their technical assistance with transmission electron microscopy. We also thank Takashi
473 Daifuku and Shin Fujiwara for their assistance in host isolation experiments and genomic analysis.
474 The authors declare that they have no conflicts of interest. This work was supported by a Grant-
475 in-Aid for Challenging Exploratory Research (grant number 26640112) from the Japan Society for
476 the Promotion of Science. The funders had no role in study design, data collection and
477 interpretation, or the decision to submit the work for publication. We would like to thank Editage
478 (www.editage.com) for English language editing.
479

480 **REFERENCES**

481 1. **Van Valen L**. 1974. Molecular evolution as predicted by natural selection. J Mol Evol
482 **3**:89–101.
483 2. **Paterson S**, **Vogwill T**, **Buckling A**, **Benmayor R**, **Spiers AJ**, **Thomson NR**, **Quail M**,
484 **Smith F**, **Walker D**, **Libberton B**, **Fenton A**, **Hall N**, **Brockhurst MA**. 2010.
485 Antagonistic coevolution accelerates molecular evolution. Nature **464**:275–278.

486 3. **Rodriguez-Valera F**, **Martin-Cuadrado A-B**, **Rodriguez-Brito B**, **Pasić L**, **Thingstad**
487 **TF**, **Rohwer F**, **Mira A**. 2009. Explaining microbial population genomics through phage
488 predation. Nat Rev Microbiol **7**:828–36.
489 4. **Breitbart M**, **Thompson L**, **Suttle C**, **Sullivan M**. 2007. Exploring the Vast Diversity of
490 Marine Viruses. Oceanography **20**:135–139.
491 5. **Weinbauer MG**, **Rassoulzadegan F**. 2004. Are viruses driving microbial diversification
492 and diversity? Environ Microbiol **6**:1–11.
493 6. **Salmond, George PC, and Peter C. Fineran.** 2015"A century of the phage: past, present and
494 future." Nat Rev Microbiol **13.12**: 777-786.
495 7. **Diana P. Baquero, Ying Liu, Fengbin Wang, Edward H. Egelman, David Prangishvili,**
496 **Mart Krupovic.** 2020. Chapter Four - Structure and assembly of archaeal viruses.
497 Advances in Virus Research. **108**:127-164.
498 8. **Prangishvili D**. 2013. The wonderful world of archaeal viruses. Annu Rev Microbiol
499 **67**:565–85.
500 9. **Prangishvili D**, **Forterre P**, **Garrett R a**. 2006. Viruses of the Archaea: a unifying view.
501 Nat Rev Microbiol **4**:837–848.
502 10. **Dy, R. L., Richter, C., Salmond, G. P., & Fineran, P. C.** 2014. Remarkable mechanisms
503 in microbes to resist phage infections. Annu rev virol **1**, 307-331.
504 11. **Janekovic D**, **Wunderl S**, **Holz I**, **Zillig W**, **Gierl A**, **Neumann H**. 1983. TTV1, TTV2
505 and TTV3, a Family of Viruses of the Extremely Thermophilic, Anaerobic, Sulfur
506 Reducing Archaebacterium Thermoproteus tenax. Mol Gen Genet **192**:39–45.
507 12. **Maaty WS**, **Ortmann AC**, **Dlakic M**, **Schulstad K**, **Hilmer JK**, **Liepold L**, **Weidenheft**
508 **B**, **Khayat R**, **Douglas T**, **Young MJ**, **Bothner B**. 2006. Characterization of the archaeal

509 thermophile Sulfolobus turreted icosahedral virus validates an evolutionary link among
510 double-stranded DNA viruses from all domains of life. J Virol **80**:7625–7635.
511 13. **Prangishvili D**, **Vestergaard G**, **Häring M**, **Aramayo R**, **Basta T**, **Rachel R**, **Garrett**
512 **RA**. 2006. Structural and Genomic Properties of the Hyperthermophilic Archaeal Virus
513 ATV with an Extracellular Stage of the Reproductive Cycle. J Mol Biol **359**:1203–1216.
514 14. **Krupovic M**, **Quemin ERJ**, **Bamford DH**, **Forterre P**, **Prangishvili D**. 2014.
515 Unification of the globally distributed spindle-shaped viruses of the Archaea. J Virol
516 **88**:2354–8.
517 15. **Mochizuki T**, **Sako Y**, **Prangishvili D**. 2011. Provirus induction in hyperthermophilic
518 archaea: characterization of Aeropyrum pernix spindle-shaped virus 1 and Aeropyrum
519 pernix ovoid virus 1. J Bacteriol **193**:5412–5419.
520 16. **Arnold HP**, **Ziese U**, **Zillig W**. 2000. SNDV, a novel virus of the extremely thermophilic
521 and acidophilic archaeon Sulfolobus. Virology **272**:409–416.
522 17. **Muskhelishvili G**, **Palm P**, **Zillig W**. 1993. SSV1-encoded site-specific recombination
523 system in Sulfolobus shibatae. MGG Mol Gen Genet **237**:334–342.
524 18. **Martin A**, **Yeats S**, **Janekovic D**, **Reiter W**, **Aicher W**, **Zillig W**. 1984. SAV1, a
525 temperate u.v.-inducible DNA virus-like particle from the archaebacterium Sulfolobus
526 acidocaldarius isolate B12. EMBO J **3**:2165–2168.
527 19. **Fusco S**, **Liguori R**, **Limauro D**, **Bartolucci S**, **She Q**, **Contursi P**. 2015. Transcriptome
528 analysis of Sulfolobus solfataricus infected with two related fuselloviruses reveals novel
529 insights into the regulation of CRISPR-Cas system. Biochimie **118**:322–332.
530 20. **Fusco S**, **She Q**, **Bartolucci S**, **Contursi P**. 2013. T(lys), a newly identified Sulfolobus
531 spindle-shaped virus 1 transcript expressed in the lysogenic state, encodes a DNA-binding

532 protein interacting at the promoters of the early genes. J Virol **87**:5926–36.

533 21. **Sako Y**, **Nomura N**, **Uchida A**, **Ishida Y**, **Morii H**, **Koga Y**, **Hoaki T**, **Maruyama T**.
534 1996. Aeropyrum pernix gen. nov., sp. nov., a Novel Aerobic Hyperthermophilic
535 Archaeon Growing at Temperatures up to 100°C. Int J Syst Bacteriol **46**:1070–1077.

536 22. **Nakagawa S**, **Takai K**, **Horikoshi K**, **Sako Y**. 2004. Aeropyrum camini ap. nov., a
537 strictly aerobic, hyperthermophilic archaeon from a deep-sea hydrothermal vent chimney.
538 Int J Syst Evol Microbiol **54**:329–335.

539 23. **Mochizuki T**, **Yoshida T**, **Tanaka R**, **Forterre P**, **Sako Y**, **Prangishvili D**. 2010.
540 Diversity of viruses of the hyperthermophilic archaeal genus Aeropyrum, and isolation of
541 the Aeropyrum pernix bacilliform virus 1, APBV1, the first representative of the family
542 Clavaviridae. Virology **402**:347–354.

543 24. **Mochizuki T**, **Krupovic M**, **Pehau-Arnaudet G**, **Sako Y**, **Forterre P**, **Prangishvili D**.
544 2012. Archaeal virus with exceptional virion architecture and the largest single-stranded
545 DNA genome. Proc Natl Acad Sci U S A **109**:13386–91.

546 25. **Daifuku T**, **Yoshida T**, **Kitamura T**, **Kawaichi S**, **Inoue T**, **Nomura K**, **Yoshida Y**,
547 **Kuno S**, **Sako Y**. 2013. Variation of the virus-related elements within syntenic genomes
548 of the hyperthermophilic archaeon aeropyrum. Appl Environ Microbiol **79**:5891–5898.

549 26. **Nomura N**, **Morinaga Y**, **Kogishi T**, **Kim EJ**, **Sako Y**, **Uchida A**. 2002. Heterogeneous
550 yet similar introns reside in identical positions of the rRNA genes in natural isolates of the
551 archaeon Aeropyrum pernix. Gene **295**:43–50.

552 27. **Zerbino DR**, **Birney E**. 2008. Velvet: Algorithms for de novo short read assembly using
553 de Bruijn graphs. Genome Res **18**:821–829.

554 28. **Tamura K**, **Dudley J**, **Nei M**, **Kumar S**. 2007. MEGA4: Molecular Evolutionary

555 Genetics Analysis (MEGA) software version 4.0. Mol Biol Evol **24**:1596–1599.

556 29. **Sugawara H**, **Ohyama A**, **Mori H**, **Kurokawa K**. Microbial Genome Annotation
557 Pipeline (MiGAP) for diverse users.

558 30. **Finn RD**, **Clements J**, **Eddy SR**. 2011. HMMER web server: Interactive sequence
559 similarity searching. Nucleic Acids Res **39**.

560 31. **Finn RD**, **Bateman A**, **Clements J**, **Coggill P**, **Eberhardt RY**, **Eddy SR**, **Heger A**,
561 **Hetherington K**, **Holm L**, **Mistry J**, **Sonnhammer ELL**, **Tate J**, **Punta M**. 2014. Pfam:
562 The protein families database. Nucleic Acids Res.

563 32. **Krogh a**, **Larsson B**, **von Heijne G**, **Sonnhammer E**. 2001. Predicting transmembrane
564 protein topology with a hidden Markov model: application to complete genomes. J Mol
565 Biol **305**:567–580.

566 33. **Carver T**, **Thomson N**, **Bleasby A**, **Berriman M**, **Parkhill J**. 2009. DNAPlotter: circular
567 and linear interactive genome visualization. Bioinforma Appl NOTE **25**:119–12010.

568 34. **Nishimura, Y., Yoshida, T., Kuronishi, M., Uehara, H., Ogata, H., & Goto, S.** 2017.
569 ViPTree: the viral proteomic tree server. Bioinformatics **33(15),** 2379-2380.

570 35. **Langmead B**, **Salzberg SL**. 2012. Fast gapped-read alignment with Bowtie 2. Nat
571 Methods **9**:357–359.

572 36. **Grissa I**, **Vergnaud G**, **Pourcel C**. 2007. CRISPRFinder: a web tool to identify clustered
573 regularly interspaced short palindromic repeats. Nucleic Acids Res **36**:52–57.

574 37. **Einen J**, **Thorseth IH**, **Øvreås L**. 2008. Enumeration of Archaea and Bacteria in seafloor
575 basalt using real-time quantitative PCR and fluorescence microscopy. FEMS Microbiol
576 Lett **282**:182–187.

577 38. **Häring M**, **Peng X**, **Brügger K**, **Rachel R**, **Stetter KO**, **Garrett RA**, **Prangishvili D**.

578 2004. Morphology and genome organization of the virus PSV of the hyperthermophilic
579 archaeal genera Pyrobaculum and Thermoproteus: A novel virus family, the
580 Globuloviridae. Virology **323**:233–242.
581 39. **Ahn DG**, **Kim S Il**, **Rhee JK**, **Pyo Kim K**, **Pan JG**, **Oh JW**. 2006. TTSV1, a new virus-
582 like particle isolated from the hyperthermophilic crenarchaeote Thermoproteus tenax.
583 Virology **351**:280–290.
584 40. **Wang H**, **Peng N**, **Shah S a**, **Huang L**, **She Q**. 2015. Archaeal Extrachromosomal
585 Genetic Elements. Microbiol Mol Biol Rev **79**:117–152.
586 41. **Iranzo J**, **Koonin E V**, **Prangishvili D**, **Krupovic M**. 2016. Bipartite network analysis of
587 the archaeal virosphere: evolutionary connections between viruses and capsid-less mobile
588 elements. J Virol **90**:11043–11055.
589 42. **Xavier Gomis-Rüth F**, **Solà M**, **Acebo P**, **Párraga A**, **Guasch A**, **Eritja R**, **González A**,
590 **Espinosa M**, **Solar G Del**, **Coll M**. 1998. The structure of plasmid-encoded
591 transcriptional repressor CopG unliganded and bound to its operator. EMBO J **17**:7404–
592 7415.
593 43. **Prangishvili D**, **Garrett RA**, **Koonin E V**. 2006. Evolutionary genomics of archaeal
594 viruses: Unique viral genomes in the third domain of life. Virus Res **117**:52–67.
595 44. **Hatfull GF**. Bacteriophage Genomics.
596 45. **Clore AJ**, **Stedman KM**. 2007. The SSV1 viral integrase is not essential. Virology
597 **361**:103–111.
598 46. **Makarova KS**, **Wolf YI**, **Alkhnbashi OS**, **Costa F**, **Shah SA**, **Saunders SJ**, **Barrangou**
599 **R**, **J Brouns SJ**, **Charpentier E**, **Haft DH**, **Horvath P**, **Moineau S**, **M Mojica FJ**,
600 **Terns RM**, **Terns MP**, **White MF**, **Yakunin AF**, **Garrett RA**, **van der Oost J**,

601 **Backofen R**, **Koonin E V**. 2015. The CRISPR–Cas modules are adaptive immune sys-
602 tems that are present in most archaea and many bacte- ria. Nat Publ Gr **13**.
603 47. **Reiter WD**, **Palm P**. 1990. Identification and characterization of a defective SSV1
604 genome integrated into a transfer-RNA gene in the archaebacterium Sulfolobus sp B12.
605 Mol Gen Genet **221**:65–71.
606 48. **Contursi P**, **Jensen S**, **Aucelli T**, **Rossi M**, **Bartolucci S**, **She Q**. 2006. Characterization
607 of the Sulfolobus host-SSV2 virus interaction. Extremophiles **10**:615–627.
608
609

610 **Figure Legends**

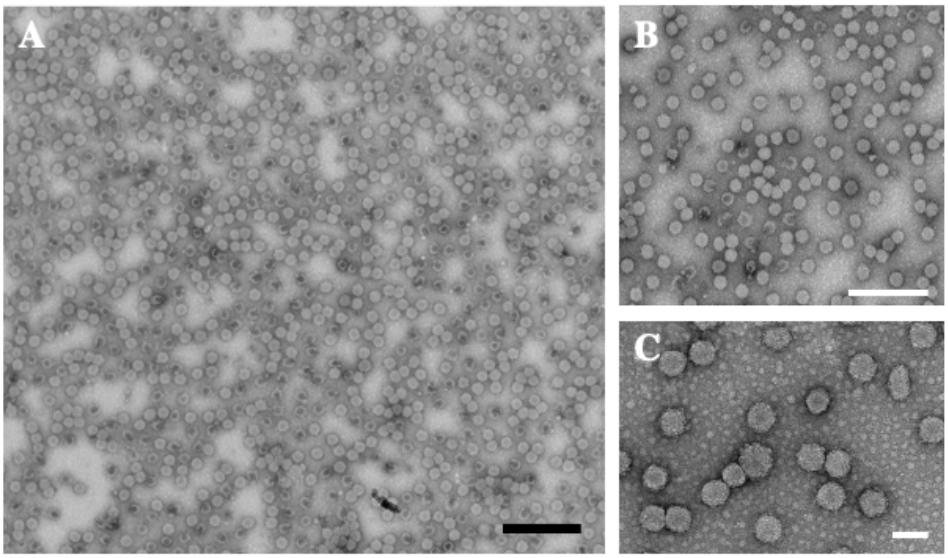

611

612 **Fig. 1 Morphology of AGV1 virions.** Representative transmission electron micrographs of virus

613 particles derived from *A. pernix* YK1-12-2013 cultures grown with buffer A. Cells are negatively

614 stained with 1% uranyl acetate. Scale bars: 500 nm (A, B) and 100 nm (C).

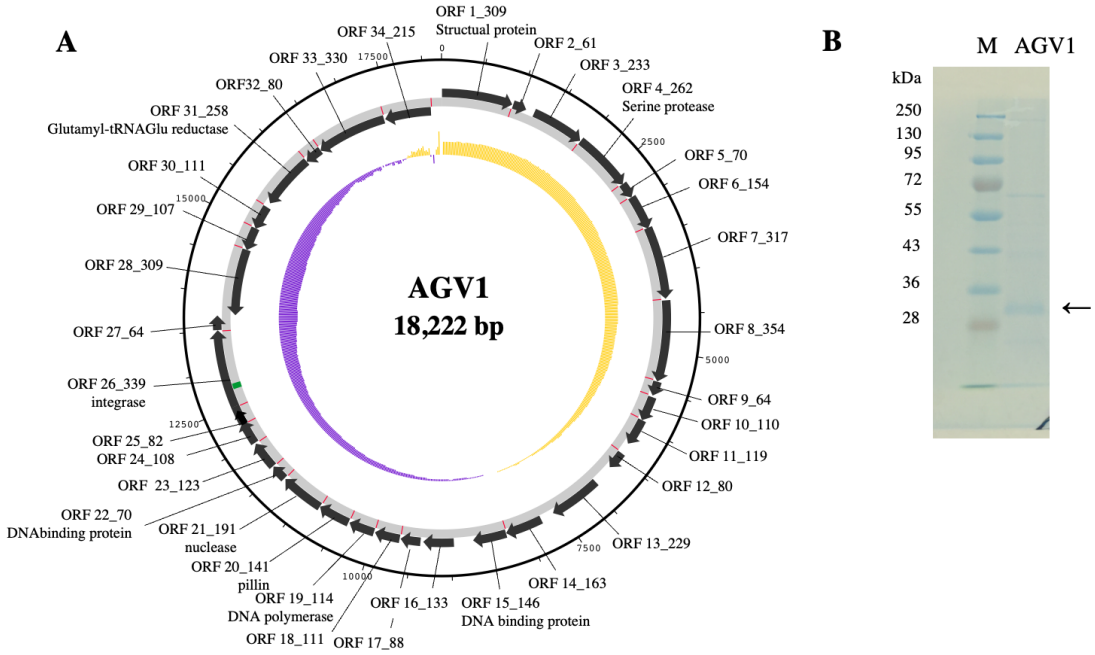
A
AGV1
18,222 bp
ORF 1_309
Structual protein
ORF 2_61
ORF 3_233
ORF 4_262
Serine protease
ORF 5_70
ORF 6_154
ORF 7_317
ORF 8_354
ORF 9_64
ORF 10_110
ORF 11_119
ORF 12_80
ORF 13_229
ORF 14_163
ORF 15_146
DNA binding protein
ORF 16_133
ORF 17_88
ORF 18_111
ORF 19_114
DNA polymerase
ORF 20_141
pillin
ORF 21_191
nuclease
ORF 22_70
DNAbinding protein
ORF 23_123
ORF 24_108
ORF 25_82
ORF 26_339
integrase
ORF 27_64
ORF 28_309
ORF 29_107
ORF 30_111
ORF 31_258
Glutamyl-tRNAGlu reductase
ORF32_80
ORF 33_330
ORF 34_215
0
2500
5000
7500
10000
12500
15000
17500
B
M
AGV1
kDa
250
130
95
72
55
43
36
28

615

C

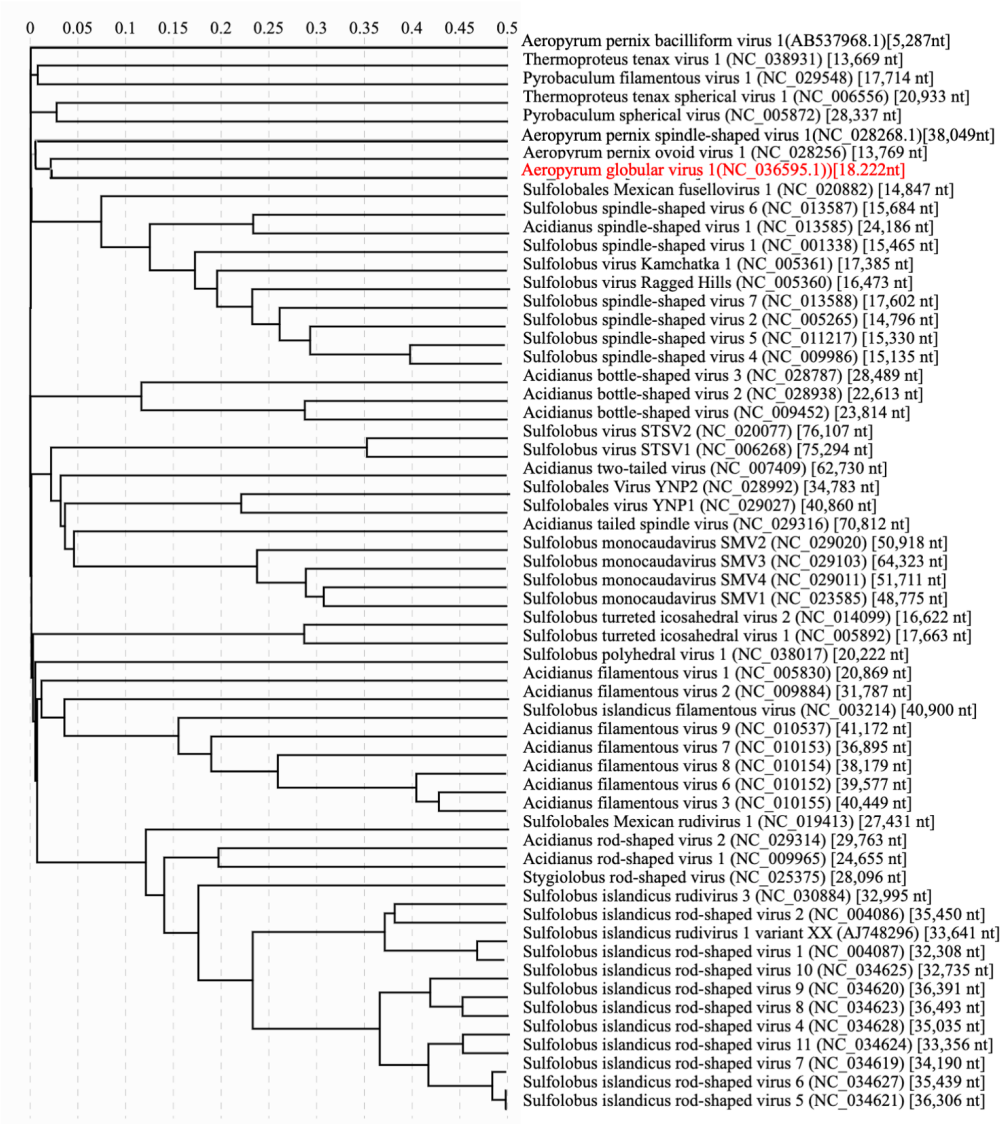

Fig. 2 Genomic information of AGV1. (A) Genome map of AGV1. Outer ring shows the genomic contents: black arrows, ORFs with strand orientation; red, ribosome-binding site; and green, $tRNA^{Glu}$ gene. Inner ring shows the GC skew (window size: 9000 and step size: 25): purple, negative GC skew; yellow, positive GC skew. Replication origin is located at the intergenic region between ORF1_309 and ORF34_215. (B) Structural protein of AGV1. Representative SDS-PAGE

622 gel shows the proteins of the virions stained with CBB stain one. Molecular mass marker (M) are

623 shown. The arrow indicates the viral major protein identified. (C) Phylogenetic tree of the genetic

624 relationship among crencarchaeal viruses based on genome-wide sequence similarities computed

625 by tBLASTx. The tree was generated by ViPTree. SG values are shown in top row.

626

627

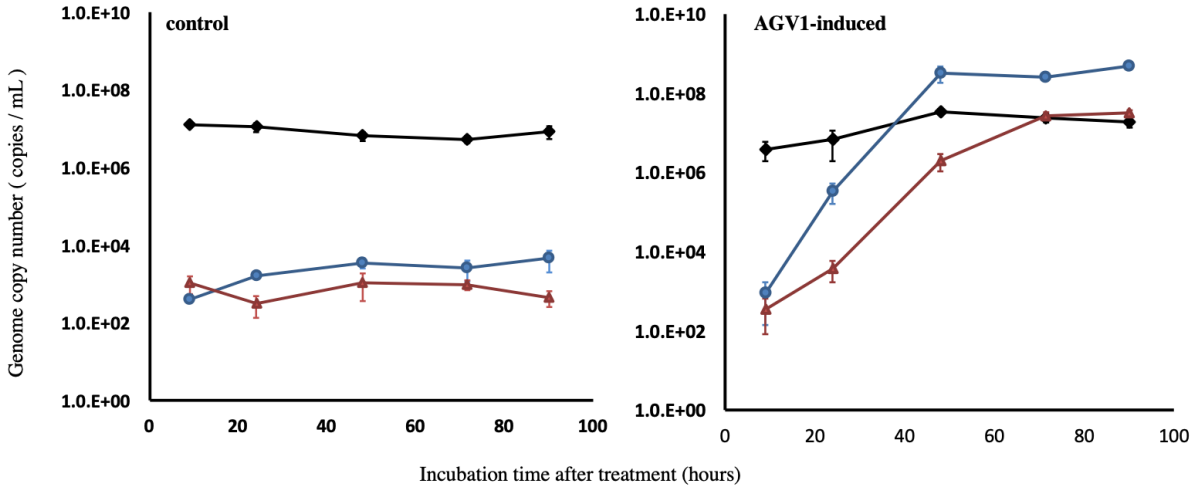

628

629 **Fig. 3 Time-course of AGV1 and host genome copy numbers.** Native host *A. pernix* YK1-12-

630 2013 was cultivated at 90ºC, and samples were collected at the indicated time points. The host

631 genome copy numbers (black diamond) and the virus genome copy numbers in the cell pellet (blue

632 circle) and supernatant (red triangle) from 10 mL culture of *A. pernix* YK1-12-2013 were measured

633 using quantitative PCR analysis of the DNA extracted from the host cells and released virions,

634 respectively. Error bars represent the mean ± SE of triplicates.

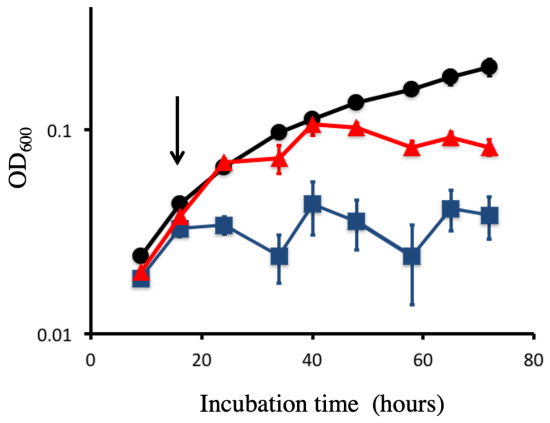

635

636 **Fig. 4 Effect of AGV1 on the growth of *A. pernix* YK1-12-2013 strain.** Black circles, red

637 triangles, and blue squares indicate the control, tris-acetate buffer-added culture, and AGV1

638 fraction-added culture. The AGV1 fraction or tris-acetate buffer was added at the time indicated

639 by the arrow. Error bars represent the mean ± SE of six replicates.

640

641

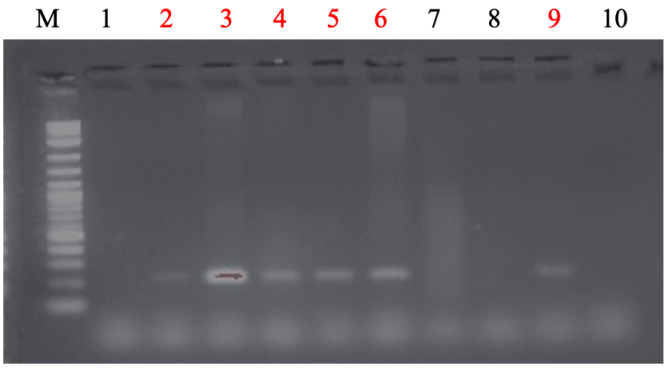

642

643 **Fig. 5 AGV1 Induction assay.** PCR analysis was performed using AGV1-specific primers to

644 confirm the kind of stress induced by AGV1 propagation. M: 2 log ladder, 1-9: YK1-12-2013

645 genome extracted from cells under various stress treatments: 1: optimal, 2: addition of 20 mM tris-

646 acetate buffer, 3: addition of 50 mM tris-acetate buffer, 4: addition of 100 mM tris-acetate buffer,

647 5: UV irradiation for 30 s, 6: suboptimal growth temperature, 7: addition of 20 mM EDTA (pH

648 7.0), 8: high salinity, 9: suboptimal growth pH, and 10: DDW (negative control). The lanes

649 confirming product amplification are in red.

650

651 **Tables**

652 **Table 1 Primers used in this study**

Primer name	Sequence (5'→3')	Length (bp)	Usage	Reference
931f	AGGAATTGGCGGGGGAGCA	19	real time PCR for 16S rDNA	Einen et al. 2008
m1100r	BGGGTCTCGCTCGTTRCC	18	real time PCR for 16S rDNA	Einen et al. 2008
IntF	AGGCCCTAGGATTCAACGGA	20	real time PCR for AGV1 integrase	This study
IntR	CACGTGACCTCAGGGTCATT	20	real time PCR for AGV1 integrase	This study

653

654

655 **Table 2 Sequence status of the host and AGV1 genomes**

Characteristics	AGV1	*A. pernix* YK1-12-2013
Genome size (bp)	18,222	1,601,052
GC content (%)	55.8	56.5
No. of contigs	1	144
Total no. of genes	35	1,772
No. of RNA genes	1	45
No. of ORFs	34	1,727

656

657

658

659 **Table 3 Summary of the predicted ORFs in the AGV1 genome**

660

	position	Length (aa)	Function	HMM predictions	BLASTP Hit	Identity (%)	*E*-value
ORF1_309	1..930	309	Structual protein*				
ORF2_61	936..1121	61					
ORF3_233	1227..1928	233					
ORF4_262	1930..2718	262	serine protease	Trypsin-like peptidase domain (aa 57-197 hit to PF13365.4; 3.6e-21)	*Pyrodictium* sp (ref|HID40799.1)	64/182(35%)	1.00E-23
ORF5_70	2708..2920	70					
ORF6_154	2913..3377	154					
ORF7_317	3361..4314	317					
ORF8_354	4329..5393	354					
ORF9_64	5390..5584	64					
ORF10_110	5600..5932	110					
ORF11_119	5925..6284	119					
ORF12_80	6427..6669	80					
ORF13_229	6927..7616	229					
ORF14_163	7784..8275	163					
ORF15_146	8272..8712	146	DNA binding (RHH)	Ribbon-helix-helix protein, copG family (aa 111-147 hit to PF1402.21; 4.6e-07)			
ORF16_133	8957..9358	133					
ORF17_88	9388..9654	88					
ORF18_111	9660..9995	111		Uncharacterized protein conserved in bacteria (aa 3-109 hit to PF09995.9; 3.2e-06)	*Aeropyrum pernix* ovoid virus 1 (ref|WP_010865925.1|)	70/111(63%)	1.00E-42
ORF19_114	10003..10347	114	DNA polymerase	DNA polymerase alpha subunit p180 N terminal (aa13-69 hit to PF12255.8; 1.8e-06)			

ORF20_141	10355..10780	141	pillin	Archaeal Type IV pilin, N-terminal (aa 4-93 hit to PF07790.11; 1.0e-08)	*Thermogladius calderae* 1633 (ref|AFK51634.1|)	59/151(39%)	9.00E-19
ORF21_191	10777..11352	191	nuclease	Viral/Archaeal nuclease (aa 22-175 hit to PF12187.8; 3.3e-13)	*Pyrodictium delaneyi* (ref|WP_082419610.1|)	75/180(42%)	2.00E-28
ORF22_70	11363..11575	70	DNA binding (RHH)	Ribbon-helix-helix protein, copG family (aa 21-58 hit to PF01402.21; 5.0e-10)	*Aeropyrum pernix* spindle-shaped virus 1 (ref|YP009177778.1|)	45/69(65%)	5.00E-24
ORF23_123	11578..11949	123					
ORF24_108	11959..12285	108		HemN C-terminal domain (aa 9-77 hit to PF06969.16; 1.9e-06)			
ORF25_82	12248..12496	82		TIR domain (aa 4-60 hit to PF13676.6; 1.4e-06)	*Aeropyrum pernix* (ref|WP_131159643.1|)	51/86(59%)	3.00E-26
ORF26_339	12493..13512	339	integrase	Archaeal phage integrase (aa 180-333 hit to PF16795.5; 2.4e-40)	*Sulfolobus* spindle-shaped virus 1 (ref|NP_039778.1|)	117/333(35%)	1.00E-44
ORF27_64	13509..13703	64					
ORF28_309	complement(13710..14639)	309	ATP binding protein	P-loop containing region of AAA domain (aa 28-65 hit to PF13555.6; 1.7e-06)	*Pyrodictium* sp.(ref:|HID41144.1|)	142/249(57%)	9.00E-93
ORF29_107	complement(14642..14965)	107					
ORF30_111	complement(14967..15302)	111					
ORF31_258	complement(15377..16153)	258	Glutamyl-tRNAGlu reductase	Glutamyl-tRNAGlu reductase, dimerisation domain (aa 64-143 hit to PF00745.20; 1.3e-06)	*Aeropyrum pernix* ovoid virus (WP_010865937.1)	189/258(73%)	2.00E-133
ORF32_80	complement(16160..16402)	80					
ORF33_330	complement(16407..17399)	330			*Thermoprotei archaeon* (ref|RLE66374.1|)	42/106(40%)	7.00E-08
ORF34_215	complement(17421..18068)	215					

661

Table 4 Comparison of spacer sequences to identify putative protospacers

Strain	Spacer or virus gene[a]	Nucleotide Sequence[b]	Predicted amino acid sequence[b]
Aeropyrum pernix K1	NC_000854_2_5*	TGAGGTTGAGGCCCGTAACAGGGCCGAGCTGGCCAGGCT	EVEARNRAELAR
	AGV1_5	||||||||||||||||||||||||||||||||||||T|||||	||||||||||||
	NC_000854_3_26	TCGAGCACTTCCAGGCCGCAGGCCTGGCCAGGCTTGAGAACGGCAG	EHFQAAGLARLENG
	AGV1_4	||||||||||||||||G||T|||||T||T|||||||||||||||||	||||||||||||||
	NC_000854_3_29 *	ATATCCACTAGGTGGTAGACCTGCGAGGCGTGGACTG	VHASQVYHLVD
	AGV1_28	|||||G|||||A|||||||||||||||||||||||||	||||||||||||
	NC_000854_3_38	TACAACTTCCTCAGGTGGCTCGCAGCATACGGCCCCGT	YNFLRWLAAYGP
	AGV1_21	|||||||||||G|||||||||||C||C|||||||||||	||||||||||||
	NC_000854_3_37	CTAGCCCCCCTGCTGGCCCTGCTCCTAG	LAPLLALLL
	AGV1_1	|||||A||||||||||||||||||||||	|||||||||
Aeropyrum pernix	CRISPR2_45	AGGAGTGCGGACTACACTACAGACCCGGATATAGGGG	RSADYTTDPDIG
YK1-12-2013	AGV1_8	|||||||||||||||||||||||||||||||||||||	||||||||||||
	CRISPR2_37*	CACGTGGTGGATACTTGCGACACTATAACAGGTGTTC	HVVDTCDTITGV
	AGV1_4	|||||||||||||||||||||||||||||||||||||	||||||||||||
	CRISPR2_35*	GGTACCAGCAGGCTGCGCAGGTTCAGCCCGCCGCCCT	GGGLNLRSLLI
	AGV1_33	||||**T**||||||||||||||||||||||||||||||||||	||||||||||**V**

a In each row, the spacer (top) and the corresponding putative protospacer (bottom) are shown.
b Identical nucleotides and amino acids are indicated by vertical lines. Nonsynonymous substitutions are shown in boldface.

* A reverse complementary sequence is shown.